Acta Pharmaceutica Sinica B 2022;12(3):1322−1338

Chinese Pharmaceutical Association
Institute of Materia Medica, Chinese Academy of Medical Sciences

Acta Pharmaceutica Sinica B

www.elsevier.com/locate/apsb
www.sciencedirect.com

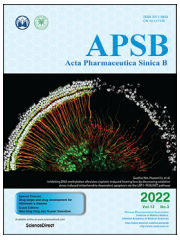

ORIGINAL ARTICLE

Anthelmintics nitazoxanide protects against experimental hyperlipidemia and hepatic steatosis in hamsters and mice

Fengfeng Li[a,b], Man Jiang[a,b], Minghui Ma[a,b], Xuyang Chen[a,b], Yidan Zhang[a,b], Yixin Zhang[a,b], Yuanyuan Yu[a,b], Yunfeng Cui[a,b], Jiahui Chen[a,b], Hui Zhao[a,b], Zhijie Sun[c,*], Deli Dong[a,b,c,*]

[a]*Department of Pharmacology (the State-Province Key Laboratories of Biomedicine-Pharmaceutics of China, Key Laboratory of Cardiovascular Research, Ministry of Education), College of Pharmacy, Harbin Medical University, Harbin 150086, China*
[b]*Translational Medicine Research and Cooperation Center of Northern China, Heilongjiang Academy of Medical Sciences, Harbin Medical University, Harbin 150086, China*
[c]*Department of Pharmacology, China Pharmaceutical University, Nanjing 211198, China*

Received 22 May 2021; received in revised form 16 July 2021; accepted 27 August 2021

KEY WORDS

Nitazoxanide;
Tizoxanide;
Hyperlipidemia;
Hepatic steatosis;
AMPK;
Autophagy;
SQSTM1/P62;
Mitochondrial uncoupling

Abstract Lipid metabolism disorders contribute to hyperlipidemia and hepatic steatosis. It is ideal to develop drugs simultaneous improving both hyperlipidemia and hepatic steatosis. Nitazoxanide is an FDA-approved oral antiprotozoal drug with excellent pharmacokinetic and safety profile. We found that nitazoxanide and its metabolite tizoxanide induced mild mitochondrial uncoupling and subsequently activated AMPK in HepG2 cells. Gavage administration of nitazoxanide inhibited high-fat diet (HFD)-induced increases of liver weight, blood and liver lipids, and ameliorated HFD-induced renal lipid accumulation in hamsters. Nitazoxanide significantly improved HFD-induced histopathologic changes of hamster livers. In the hamsters with pre-existing hyperlipidemia and hepatic steatosis, nitazoxanide also showed therapeutic effect. Gavage administration of nitazoxanide improved HFD-induced hepatic steatosis in C57BL/6J mice and western diet (WD)-induced hepatic steatosis in *Apoe*$^{-/-}$ mice. The present study suggests that repurposing nitazoxanide as a drug for hyperlipidemia and hepatic steatosis treatment is promising.

*Corresponding authors.
E-mail addresses: dongdeli@ems.hrbmu.edu.cn (Deli Dong), sunzhijie@cpu.edu.cn (Zhijie Sun).

Peer review under responsibility of Chinese Pharmaceutical Association and Institute of Materia Medica, Chinese Academy of Medical Sciences.

https://doi.org/10.1016/j.apsb.2021.09.009

1. Introduction

Lipid metabolism disorders contribute to numerous diseases including hyperlipidemia, atherosclerosis and metabolic dysfunction-associated fatty liver disease (MAFLD), which cause heavy medical and financial burdens worldwide[1,2]. Lipid metabolism disorders encompass abnormal levels of lipids and their metabolites in plasma or related organ/cells. The role of lipid metabolism disorders in the pathogenesis of atherosclerosis and MAFLD has been well reviewed[3,4]. It is no doubt that lipid lowering agents reduce not only atherosclerosis but also cardiovascular events[5,6]; however, MAFLD cannot be simply cured by lowering blood or liver lipids. Statins have always been the first-line pharmacological treatment for hyperlipidemia, but they are not clinical drugs for MAFLD. Nevertheless, the drugs such as telmisartan and pentoxifylline which have benefit for MAFLD in clinic trials do not belong to the lipid-lowering agents[7,8]. Recent studies even show that inhibition of acetyl-CoA carboxylase reduces liver triglycerides but increases plasma triglycerides in rodents and humans[9,10]. Therefore, for the pharmacological therapy of MAFLD, it will be ideal to develop the drugs that not only lower liver and plasma lipid, but also improve the pathology of MAFLD.

Nitazoxanide is an FDA-approved oral antiprotozoal drug with good bioavailability and safety profile. Since 2004, it has been further clinically applied for the treatment of *Giardia*- and *Cryptosporidium*-associated diarrhea in adults and children[11]. Recent studies show that nitazoxanide is also a broad-spectrum antiviral agent[12,13]. Nitazoxanide is *in vivo* metabolized to tizoxanide. Both nitazoxanide and tizoxanide have the similar chemical structure with another antihelminthic drug niclosamide[13] (Supporting Information Fig. S1). Niclosamide is a mitochondrial uncoupler and has been proven to prevent hepatic steatosis induced by high-fat diet in mice due to its mild uncoupling effect[14]. The similar chemical structure shared by niclosamide, tizoxanide and nitazoxanide enlightens us to hypothesize that nitazoxanide might induce mild mitochondrial uncoupling in hepatic cells and improve hyperlipidemia and MAFLD. In the present study, we demonstrate that nitazoxanide and its metabolite tizoxanide activate AMPK in HepG2 cells through inducing mild mitochondrial uncoupling and gavage administration of nitazoxanide protects against experimental hyperlipidemia and hepatic steatosis in hamsters and mice. Nitazoxanide has been the clinical drug for parasitic worms and *Giardia*- and *Cryptosporidium*-associated diarrhea treatment, our present work suggests a promising translation for the old drug to be used for hyperlipidemia and MAFLD in clinic.

2. Materials and methods

2.1. Cell culture and reagents

HepG2 cells (Human hepatoblastoma cell line) and LO2 cells (Normal human hepatic cell line) were purchased from Zhongqiaoxinzhou Biotech (Shanghai, China). HepG2 cells were cultured in Dulbecco's modified Eagle's medium (DMEM, Hyclone, UT, USA) supplemented with 10% fetal bovine serum (FBS, Biological Industries, Beit Haemek, Israel) and 1% penicillin/streptomycin (P/S, Solarbio, Beijing, China) and LO2 cells were cultured in Roswell Park Memorial Institute 1640 medium (RPMI-1640, Hyclone, UT, USA) supplemented with 10% FBS and 1% P/S. All cells were cultured at 37 °C and 5% CO_2 atmosphere. Nitazoxanide (Nit) was purchased from Adamas-beta (Shanghai, China). Tizoxanide (Tiz), compound C, and chloroquine were obtained from MedChemExpress (NJ, USA). Niclosamide (Nic) was purchased from Jianglai Reagent Company (Shanghai, China). Atorvastain calcium was bought from Pfizer (New York, NY, USA). The antibodies used for Western blot are as follows: p-AMPKα^{Thr172} (#2535, CST, MA, USA), AMPKα1 (#bsm-33338M, Bioss ANTIBODIES, Beijing, China), p-ACC^{Ser79} (#11818, CST), ACC (#3676, CST), LC3A/B (#AF5402, Affinity Biosciences, Changzhou, China), LC3B (#L7543, Sigma−Aldrich, St Louis, MO, USA), SQSTM1/P62 (#P0067, Sigma−Aldrich), TFEB (#A303-673A, Bethyl Laboratories Inc., TX, USA), β-actin (#AC026, Abclonal, Wuhan, China), GAPDH (#AC002, Abclonal), Lamin B1 (#A1910, Abclonal), goat anti-mouse IgG (#926−32210, LI-COR Biosciences, Lincoln, NE, USA) and goat anti-rabbit IgG (#926−32211, LI-COR Biosciences).

2.2. Animal diets

The high-fat diet (HFD), bought from hfkbio (Beijing, China), consists of 10% lard, 15% sucrose, 15% yolk powder, 5% casein, 1.2% cholesterol, 0.2% sodium cholate, 0.6% dibasic calcium phosphate, 0.4% calcium carbonate and 52.6% standard chow diet. Western diet (WD) was purchased from hfkbio (Beijing, China), it contains 34.1% sucrose, 20% anhydrous butter, 19.5% casein, 10% maltodextrin, 5% corn starch, 5% cellulose, 1% corn oil, 0.3% methionine, 0.4% calcium carbonate, 0.2% choline bitartrate, 3.5% mineral mixture, 1% vitamin mixture and extra 0.15% cholesterol.

2.3. Animal maintenance and experiments

All animal care and experimental protocols for this study complied with the Laboratory Animal Management Regulations in China and were approved by the Institutional Animal Care and Use Committee of Harbin Medical University, China. Animal studies are reported in compliance with the ARRIVE guidelines[15,16].

Specific pathogen-free (SPF) male golden Syrian hamsters (110−130 g, 5 weeks old) and male C57BL/6J mice (20−23 g, 8 weeks old) were supplied by Changsheng Biotechnology (Liaoning, China), SPF male *Apoe*$^{-/-}$ mice (23−27 g, 8 weeks old) mice with a C57BL/6J background and weight-matched wild type (WT) mice were purchased from hfkbio (Beijing, China). All animals were in good health conditions and maintained in a temperature-controlled environment at 23 ± 1 °C under a 14-h light/10-h dark circadian rhythm with free access to water and food. After

acclimatization for a week, the animals were randomly assigned to experimental groups.

To induce hyperlipidemia and hepatic steatosis model, hamsters were fed a high-fat diet (HFD, 40.29% fat calories, hfkbio, Beijing, China) for 50 days. Nitazoxanide (Nit, 50, 100, and 200 mg/kg/day) and atorvastatin (Ato, 1.2 mg/kg/day) were gavaged continuously. The normal diet (ND) control group and the HFD model group were treated with an appropriate volume of solvent (0.5% methylcellulose).

For the study of whether nitazoxanide treatment could ameliorate the pre-existing hyperlipidemia and hepatic steatosis, an additional reversal experiment of hamsters was carried out. Hamsters fed with HFD or ND for 25 days were partially sacrificed to confirm the model establishment, then the remaining HFD-fed hamsters were randomly divided into two groups, each of which received vehicle or nitazoxanide (100 mg/kg/day) for consecutive 25 days.

C57BL/6J mice were fed HFD (40.29% fat calories, hfkbio, Beijing, China) for 16 consecutive weeks to establish hepatic steatosis mouse model, and the mice received an ND (normal diet) were as controls. Two doses of nitazoxanide (50, and 100 mg/kg/day) or solvent (0.5% methylcellulose) were administrated simultaneously by gavage during the HFD exposure.

Apoe$^{-/-}$ mice were divided into four groups and allocated into either a western diet (WD, 41% fat calories, hfkbio, Beijing, China) or a WD supplemented with gavage administration of nitazoxanide (100 and 200 mg/kg/day) and atorvastatin (2 mg/kg/day), while WT mice fed a normal diet were as control group. The groups of WT + ND and *Apoe*$^{-/-}$ + WD orally received an equal volume of solvent (0.5% methylcellulose) for 15 weeks until the mice were sacrificed. To further induce more severe hepatic steatosis symptoms in *Apoe*$^{-/-}$ mice, an additional experiment with longer duration was carried out with three groups: WT + ND, *Apoe*$^{-/-}$ + WD and *Apoe*$^{-/-}$ + WD + Nit (100 mg/kg/day) for 21 weeks.

2.4. Cell viability

The cell viability was assessed *via* an MTT assay as described in our previous studies[17–19]. HepG2 cells were deposited in 96-well flat-bottom culture plates (5×10^3 cells/well), and exposed to various concentrations of nitazoxanide (Nit, 01088480, Adamas-beta, Shanghai, China) or tizoxanide (Tiz, HY-12687, MedChemExpress, USA) for 24 h. Media were then removed, 100 μL of 0.5 mg/mL MTT (M1025, Solarbio, Beijing, China) was added to each well. After 4 h incubation, the MTT reagent was discarded, and 180 μL of dimethyl sulfoxide (DMSO, BS087, Biosharp, Hefei, China) was added to dissolve the insoluble purple formazan product. The absorbance was then measured with Tecan Infinite M200PRO Multimode Plate Reader (Switzerland) at a wavelength of 490 nm.

2.5. Live and dead cell staining

The live and dead cells were detected by using the Viability/Cytotoxicity Assay Kit (L3224; Invitrogen, OR, USA) as described in our previous studies[17–19]. Briefly, HepG2 cells seeded in six-well plate were incubated with a mixture of two dyes: 2 μmol/L Calcein-AM and 4 μmol/L EthD-1 for 15 min at 37 °C. Images of stained cells were captured under Olympus BX53 fluorescence microscope (Japan) equipped with a DP80 camera. Living cells were labeled green with Calcein-AM, while cells labeled red by EthD-1 were considered dead. Quantification of the Live/Dead cells was performed using ImagePro Plus image analysis software (Media Cybernetics Inc., MD, USA).

2.6. Mitochondrial respiratory measurements

HepG2 cells harvested *via* trypsin digestion were centrifuged by high speed refrigerated micro centrifuge (MX-307, TOMY, Tokyo, Japan) at 800 rpm for 5 min at room temperature and resuspended in culture medium. The intact whole cell respiratory function was determined by high-resolution respirometry (Oxygraph-2k, Oroboros Instruments, Innsbruck, Austria) with a well-established protocol designed as oligomycin (Omy)-uncoupler-inhibitor titrations[17,19]. Briefly, routine respiration was followed by oligomycin (0.5 μmol/L, 495455, Sigma−Aldrich) titration to induce the non-phosphorylating leak state. When respiration was stable, manual titrations of DMSO, nitazoxanide, tizoxanide, and FCCP (C2920, Sigma−Aldrich) were in steps of 1 μL for 4 times to gradually increase the final concentrations at 120 s intervals. The final concentrations of nitazoxanide and tizoxanide of each step were 1, 5, 10, and 25 μmol/L, respectively, while the concentrations of FCCP, a positive control were 0.1, 0.2, 0.5, and 1 μmol/L. DMSO was used as a solvent control. Then, rotenone and antimycin A were used to get the residual respiration.

2.7. Mitochondrial membrane potential

Mitochondrial membrane potential of cells was determined by using tetramethyl rhodamine methyl ester (TMRM) staining as described in our previous study[19]. Cultured HepG2 cells at 60% confluency were pre-treated with Nit or Tiz for 24 h, and then loaded with TMRM (50 nmol/L, Invitrogen) for 45 min and Hoechst 33,342 (10 μg/mL, C0031, Solarbio, Beijing, China) for 15 min at 37 °C. After rinsing three times with DMEM (37 °C), the fluorescence was detected by a fluorescence microscope (Olympus BX53 with DP80 camera, Japan) with 20 × objective lens. Membrane potential level was represented by relative intensity of the fluorescence.

2.8. Cellular ATP and ADP assay

The cellular ATP and ADP/ATP ratio were measured as described in our previous study[20]. To measure the ATP content, the cells were extracted on ice with the lysis buffer from ATP Assay Kit (S0026, Beyotime, China), and protein content of the samples was measured by BCA Protein Assay Kit (P0010, Beyotime). In addition, the ADP/ATP ratio was measured with the cells ($\times 10^5$/cm^3) which were harvested *via* trypsin digestion and resuspended in the lysis buffer from ADP/ATP-Lite Assay Kit (T008, Vigorous bio, Beijing, China). All the numbers of relative light units were read immediately using a luminometer (Tecan Infinite M200PRO, Switzerland).

2.9. Real-time quantitative reverse transcription PCR (RT-PCR)

Total RNA from cultured HepG2 cells was isolated using the TRIzol reagent and the quality of the extracted total RNA samples was checked by NanoDrop 8000 (Thermo, USA). For each sample, 1 μg total RNA was reverse-transcribed into cDNA using a ReverTra Ace qPCR RT Master Mix with gDNA Remover (FSQ-301, TOYOBO, Japan). For quantitative real-time PCR, the cDNA was amplified with a SYBR Green Realtime PCR Master Mix (QPK-201, TOYOBO, Japan)) at the following conditions: 95 °C/

30 s, followed by 95 °C/5 s, 50 °C/10 s and 72 °C/30 s for 40 cycles using an Applied Biosystems 7500 Fast Real-Time PCR System (Applied Biosystems, USA). Relative gene expression was calculated using the $2^{-\Delta\Delta CT}$ quantification formula normalizing with the expression of the housekeeping gene β-actin. The primer sequences are listed as follows: *SQSTM1/P62*−F, 5′-GACTACG ACTTGTGTAGCGTC-3′; *SQSTM1/P62*-R, 5′-AGTGTCCGTGT TTCACCTTCC-3′; β-actin-F, 5′-CATGTACGTTGCTATCCAGG C-3′; β-actin-R, 5′-CTCCTTAATGTCACGCACGAT-3′.

2.10. Immunofluorescence

HepG2 cells cultured on glass dishes were pre-treated with Nit or Tiz (10 μmol/L) in the absence or presence of compound C (CC, 10 μmol/L, HY-13418A, MedChemExpress, USA) for 24 h. After being washed with PBS for 3 times, cells were subsequently fixed with 4% paraformaldehyde for 15 min, penetrated in PBS containing 0.4% Triton X100 for 1 h and blocked with goat serum (AR0009, Boster Biotech Technology, USA) for 30 min at room temperature. For monitoring nuclear translocation of TFEB, cells were then incubated with TFEB antibody (dil:1:200, A303-673A, Bethyl Laboratories Inc., USA) overnight at 4 °C, followed by incubation with the secondary antibody conjugated to Alexa Fluor 594 (dil:1:400, A-11037, Invitrogen) for 1 h, and the nuclei were counterstained with DAPI (10 μg/mL, C0065, Solarbio, Beijing, China) for 15 min. Fluorescence images were acquired by using a FV10i confocal microscope (OLYMPUS, Japan).

2.11. Cytoplasmic and nuclear protein extraction

Cytoplasmic and nuclear proteins were extracted from HepG2 cells using the Nuclear and Cytoplasmic Protein Extraction Kit (P0028, Beyotime, China) according to the manufacturer's protocols. In brief, the 200 μL of reagent A containing 1% PMSF (P0100, Solarbio, Beijing, China) was added to the harvested cell pellet (20 mm^3). The mixture was vortexed vigorously for 5 s and incubated on ice for 15 min. After being injected by 10 μL reagent B and vortexed for 5 s, the mixture was further incubated on ice for 1 min and then centrifuged by high speed refrigerated micro centrifuge (MX-307, TOMY, Tokyo, Japan) at 4 °C for 5 min at 14,000 rpm. The resultant supernatant was collected as the cytoplasmic protein extract. The pellet was washed with PBS twice and mixed with 50 μL nuclear protein extraction reagent. The mixture was incubated on ice for 30 min during which it subject to 30 s of vortex every 2 min. Lastly, the suspension was centrifuged at 4 °C for 10 min at 14,000 rpm and the supernatant was collected as the nuclear fraction. Fractions were subsequently determined by Western blot analysis.

2.12. Temperature measurement

After intraperitoneal anesthesia with 10% chloral hydrate, the anus temperatures of the animals were measured by a thermometer (JNT-LGJ, Nuo Tai Technology, Beijing, China).

2.13. Hepatic lipid analysis

Commercial kits were used to measure the liver triglyceride (TG) and total cholesterol (TC) according to the manufacturer's instructions (E1025-105T for TG, E1026-105T for TC, Applygen, Beijing, China). Briefly, the liver tissues were lysed with lysate in the kits. After centrifugation at 2000×*g* for 5 min, the supernatants were used to determine the TG and TC concentrations. And the liver tissue protein concentrations, assessed by BCA Protein Assay Kit (P0010, Beyotime, China), were used for calibration.

2.14. Serum assays

Serum was isolated from the blood samples which had already been rested at room temperature for 4 h *via* centrifugation (4000×*g*, 15 min). The levels of serum total cholesterol (TC), triglycerides (TG), high density lipoprotein cholesterol (HDL-C), low density lipoprotein cholesterol (LDL-C), aspartate aminotransferase (AST), and alanine transaminase (ALT) were analyzed by enzymatic colorimetric methods using reagent kits (E1003-250 for TG, E1005-250 for TC, Applygen, Beijing, China; A112-1-1 for HDL-C, A113-1-1 for LDL-C, c010-2-1 for AST, c009-2-1 for ALT, njjcbio, Nanjing, China) following the instructions. The measured parameters were detected by Tecan Infinite M200PRO Multimode Plate Reader (Switzerland) or Molecular Devices CMax Plus (CA, USA).

2.15. Histopathologic analysis

For histopathologic analysis, hematoxylin−eosin (H&E) staining was performed using paraffin-prepared liver, kidney and white adipose tissue sections (5 μm). In addition, frozen liver and kidney tissues embedded with O.C.T Compound (Sakura Finetek USA Inc., Torrance, CA, USA) were cut into sections of 10 μm thickness, and then stained with oil red O staining solution (Sangon Biotech, Shanghai, China) to evaluate the degree of lipid deposition. Images were obtained using a light microscope (Olympus BX53 with DP80 camera, Japan) at 200× magnification.

2.16. Western blotting

Protein samples from cultured cells and animal tissues were harvested with RIPA buffer containing 1% protease inhibitor and 10% phosphatase inhibitor. After quantification by BCA Protein Assay Kit (P0010, Beyotime), equal amounts of protein were separated by electrophoresis on 7.5%−12.5% SDS-PAGE gels (PG111, PG112, PG113, Epizyme Biotech, Shanghai, China) and blotted onto nitrocellulose membranes. We used 5% skim milk as the blocking buffer and TBS−0.1% Tween 20 as washing buffer. After incubation with the primary antibody at 4 °C overnight, the membranes were subsequently incubated with fluorescence-labeled secondary antibodies (LI-COR Biosciences, Lincoln, NE, USA) for 1 h. The images were scanned by the Odyssey CLx Infrared Imaging System (LI-COR Biosciences, Lincoln, NE, USA) and the bans were quantified with Image Studio 5.0 software (LI-COR Biosciences, Lincoln, NE, USA).

2.17. Quantification and statistical analysis

All data were expressed as mean ± standard error of mean (SEM) and analyzed by using GraphPad Prism version 7.0 (GraphPad Software Inc., San Diego, CA, USA). Statistical significance of two groups was determined with Student's *t*-test. For two more groups, one-way ANOVA or two-way ANOVA followed by Dunnett test or Tukey's test was used. For the data with control value of 1 and no SEM, the randomized block ANOVA (repeated measures ANOVA) was used. $P < 0.05$ was considered statistically significant.

3. Results

3.1. Nitazoxanide and its metabolite tizoxanide induce mild mitochondrial uncoupling and subsequently activate AMPK in HepG2 cells

In the present work, we used HepG2 cells in the *in vitro* experiments because the cell line possesses typical functions of the normal human hepatocytes including lipoprotein and apolipoprotein synthesis, and is widely used in the studies related to lipid metabolism[21−23]. Firstly, we examined whether nitazoxanide and its metabolite tizoxanide had mitochondrial uncoupling effect in HepG2 cells. As shown in Fig. 1A and B, both nitazoxanide and tizoxanide (1, 5, 10, and 25 μmol/L) dose-dependently enhanced mitochondrial oxygen consumption rate (OCR) of HepG2 cells, similarly to the effect of FCCP, a typical mitochondrial uncoupler. Another characterization of mitochondrial uncoupling is a decrease of mitochondrial membrane potential of cells. HepG2 cells were treated with different concentrations of nitazoxanide and tizoxanide for 24 h, then the mitochondrial membrane potential was assayed by using TMRM staining. As shown in Fig. 1C and D, both nitazoxanide and tizoxanide reduced the cellular mitochondrial membrane potential with similar potency (IC_{50} ~5.85 μmol/L). Taken together, nitazoxanide and its metabolite tizoxanide had mitochondrial uncoupling effect in HepG2 cells, consistent with the previous report that nitazoxanide induced uncoupling effect in human dopaminergic cells[24].

Mitochondrial uncoupling leads to a reduction of cellular ATP level. We further examined the effect of nitazoxanide and tizoxanide on cellular ATP level and the ADP/ATP ratio in HepG2 cells. As shown in Supporting Information Fig. S2A and S2B, both nitazoxanide and tizoxanide reduced the cellular ATP level and increased ADP/ATP ratio in HepG2 cells in a dose-dependent manner. Decrease of ATP level or increase of ADP/ATP ratio leads to AMPK activation. Then, we examined the effect of nitazoxanide and tizoxanide on AMPK activity in HepG2 cells. As shown in Fig. 1E, both nitazoxanide and tizoxanide dose-dependently activated AMPK in HepG2 cells. Acetyl-CoA carboxylase (ACC) is the substrate of AMPK and is inactivated through reversible phosphorylation by AMPK. Inhibition of ACC by AMPK leads to increased fatty acid oxidation and decreased lipid biosynthesis. Nitazoxanide and tizoxanide increased phosphorylation of ACC in HepG2 cells (Fig. 1F). In another human hepatic LO2 cells, nitazoxanide and tizoxanide also showed activating effect on AMPK (Supporting Information Fig. S3). Meanwhile, niclosamide with the similar chemical structure of nitazoxanide and tizoxanide has been reported to improve hepatic steatosis and insulin resistance through AMPK actiavtion[14]. Here, niclosamide-induced AMPK activation in HepG2 cells was further confirmed in the present experiment conditions (Supporting Information Fig. S4). These results indicate that nitazoxanide would be potentially therapeutic for lipid metabolism disorders.

Activated AMPK promotes cellular autophagy through direct or indirect pathways[25] and autophagy induction ameliorates steatohepatitis[26,27]. Previous studies reported that nitazoxanide stimulated autophagy in MCF-7 cells and primary cortical astrocytes[28,29]. Herein, we examined the effect of nitazoxanide and tizoxanide on autophagy response of HepG2 cells. As shown in Supporting Information Fig S5, both nitazoxanide and tizoxanide treatment significantly increased the protein levels of LC3-II and P62 and the ratio of LC3-II/LC3-I. Both nitazoxanide and tizoxanide treatment also increased *SQSTM1/P62* mRNA level in HepG2 cells (Supporting Information Fig. S6). P62 is generally regarded as a marker of autophagic flux because it is degraded by autophagy[30]. However, it has been reported that AMPK-induced TFEB (transcription factor EB) activation increases P62 expression[26] and TFEB-induced increase of P62 protein expression is not reduced in autophagy process[31,32]. Firstly, we proved that AMPK inhibitor compound C inhibited nitazoxanide- and tizoxanide-induced AMPK activation in HepG2 cells (Supporting Information Fig. S7A), then demonstrated that nitazoxanide and tizoxanide treatment increased TFEB nuclear translocation which was inhibited by compound C (Fig. S7B−S7E), explaining the increased SQSTM1/P62 expression in HepG2 cells (Figs. S5 and S6). The lysosomal inhibitor chloroquine (CQ) treatment further increased nitazoxanide and tizoxanide-induced increase of LC3-II protein level and LC3-II/LC3-I ratio (Supporting Information Fig. S8). The above data demonstrate that both nitazoxanide and tizoxanide induced autophagy flux in HepG2 cells.

3.2. Cytotoxicity of nitazoxanide and tizoxanide in HepG2 cells in vitro

Although it has been reported that mild mitochondrial uncoupling was protective against multiple disorders[19,33−35], excessive uncoupling was definitely harmful. We further examined the cytotoxicity of nitazoxanide and tizoxanide at the concentrations of AMPK activation in HepG2 cells. Nitazoxanide and tizoxanide slightly reduced the cell viability of HepG2 cells at the concentrations ranged from 5 to 25 μmol/L as evaluated by MTT assay (Supporting Information Fig. S9A), but the optic photographs did not show the apparent cytotoxicity except the decreased cell density at 10 and 25 μmol/L of nitazoxanide and tizoxanide (Fig. S9B). The LIVE/DEAD cell staining results show that nitazoxanide and tizoxanide only at 25 μmol/L increased cell death (Fig. S9C). These data demonstrate that it was not due to the non-specific cytotoxicity that nitazoxanide and tizoxanide induced mitochondrial uncoupling and AMPK activation in HepG2 cells at concentrations less than 25 μmol/L. These results are also in line with a recent report that nitazoxanide induced cell cycle arrest in colorectal cancer cells[36].

3.3. Gavage administration of nitazoxanide prevents high-fat diet (HFD)-induced hyperlipidemia and hepatic steatosis in hamsters

The Syrian golden hamsters have been widely used in the studies about lipid metabolism disorders because they resemble human beings in lipid utilization and lipoprotein metabolism[37−39]. We established an HFD-induced hyperlipidemia and hepatic steatosis model in hamsters, and nitazoxanide was gavaged to the hamsters at the doses equivalent to those used in clinical trials for chronic hepatitis B and chronic hepatitis C therapy (Fig. 2A)[40,41]; meanwhile, atorvastatin at the dose equivalent to clinical usage was used as a positive control (Fig. 2A). The average body weight and food intake of hamsters in each group during the period of treatment (50 days) are shown in Fig. 2B. There was no difference of body temperature among the groups (Fig. 2C). HFD feeding for 50 days induced hyperlipidemia in hamsters and both nitazoxanide and atorvastatin treatment significantly improved the

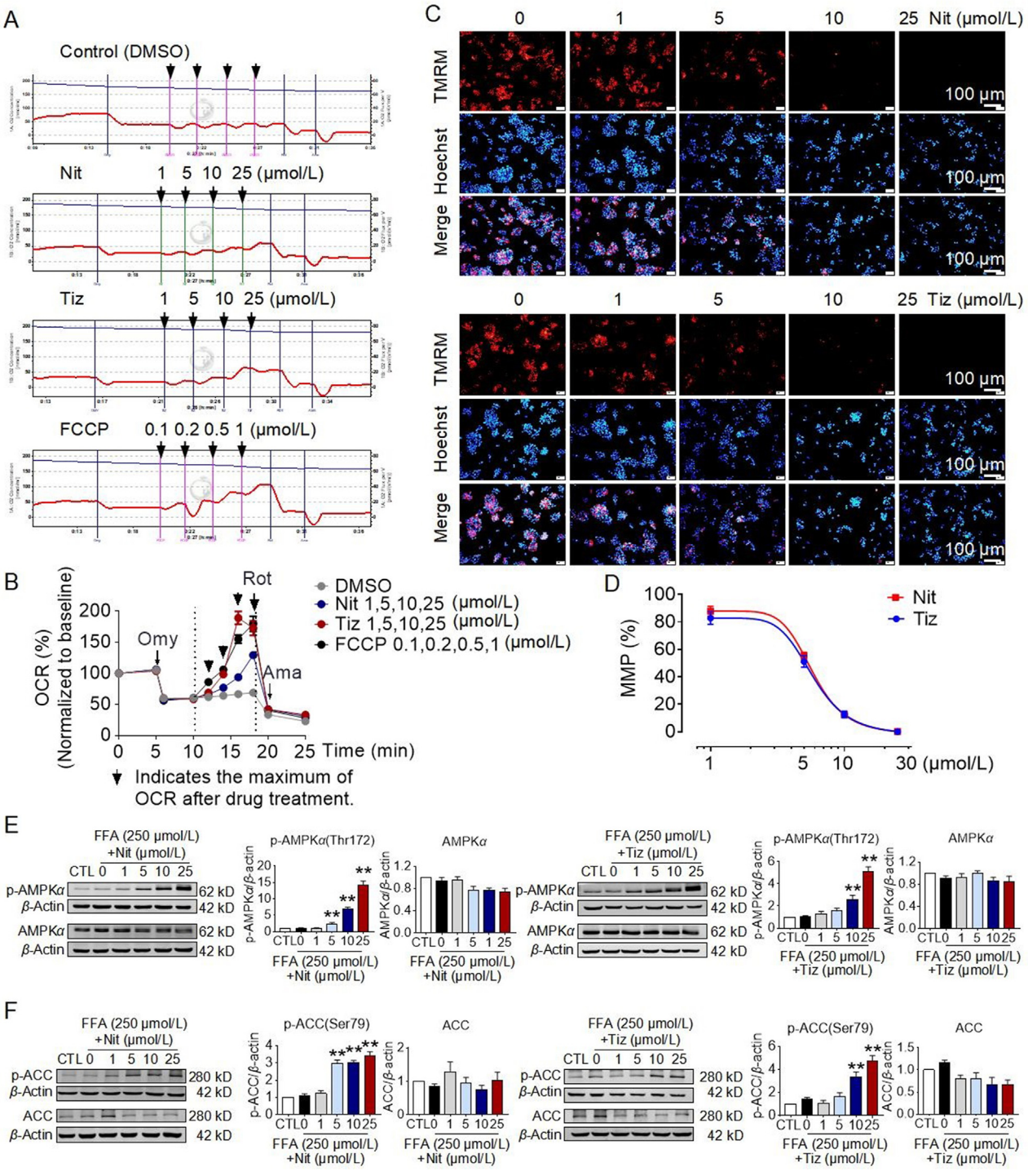

Figure 1 Nitazoxanide and tizoxanide induce mild mitochondrial uncoupling and subsequently activate AMPK in HepG2 cells. (A, B) Nitazoxanide and tizoxanide dose-dependently enhanced mitochondrial oxygen consumption rate (OCR) of HepG2 cells. The representative original recordings of OCR are shown in (A) and the analyzed data are shown in (B). FCCP was as positive control. $n = 6$ in DMSO group, $n = 7$ in nitazoxanide group, $n = 8$ tizoxanide group, $n = 7$ in FCCP group. (C, D) Nitazoxanide and tizoxanide reduced mitochondrial membrane potential of HepG2 cells. HepG2 cells were treated with different concentrations of nitazoxanide and tizoxanide for 24 h, then the mitochondrial membrane potential was assayed by using TMRM staining. The representative images of TMRM staining are shown in (C) and the analyzed data are shown in (D). $n = 6$ in each group. (E) Nitazoxanide and tizoxanide activated AMPK in HepG2 cells. HepG2 cells were stimulated with free fatty acids (FFA, 250 μmol/L) for 24 h then treated with different concentrations of nitazoxanide and tizoxanide for 24 h $n = 6$ in each group. (F) Nitazoxanide and tizoxanide increased phosphorylation of ACC in HepG2 cells. HepG2 cells were stimulated with free fatty acids (FFA, 250 μmol/L) for 24 h then treated with different concentrations of nitazoxanide and tizoxanide for 24 h $n = 6$ in each group. Data are presented as mean ± SEM. Statistical analysis was performed with the randomized block ANOVA (repeated measures ANOVA). $^{**}P < 0.01$ *vs.* CTL (control). Nit, nitazoxanide; Tiz, tizoxanide.

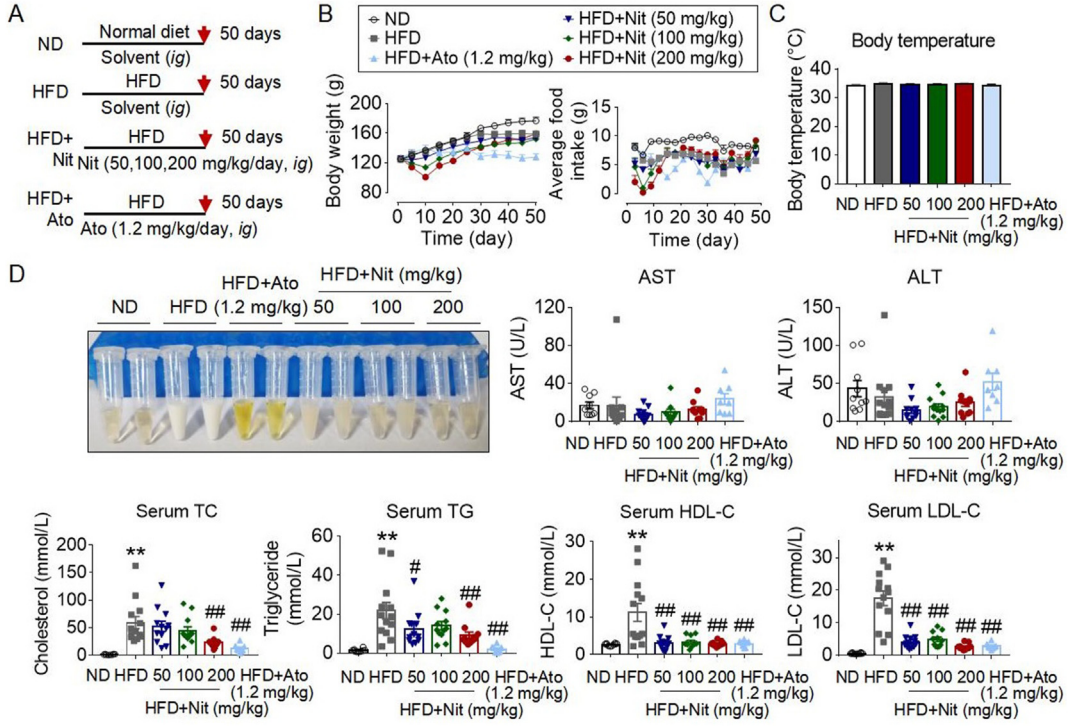

Figure 2 Gavage administration of nitazoxanide prevents HFD feeding-induced hyperlipidemia in hamsters. (A) Schematic illustration of the experiment design. (B) The time course of body weight and average food intake changes. The food intake every three days was averaged. (C) Body temperature of animals. The anus temperature of animals anesthetized with 10% chloral hydrate were measured by using a thermometer. (D) Nitazoxanide reduced the elevated blood lipids induced by HFD feeding in hamsters. TC, total cholesterol; TG, triglyceride. HDL-C, high density lipoprotein cholesterol; LDL-C, high density lipoprotein cholesterol; AST, aspartate aminotransferase; ALT, alanine aminotransferase. Data are presented as mean ± SEM; n = 10, 13, 12, 12, 11, and 9 in ND, HFD, HFD + Nit (50 mg/kg), HFD + Nit (100 mg/kg), HFD + Nit (200 mg/kg), and HFD + Ato (1.2 mg/kg) groups, respectively. Statistical analysis was performed with one-way ANOVA. $^{*}P < 0.05$, $^{**}P < 0.01$ *vs*. ND; $^{\#}P < 0.05$, $^{\#\#}P < 0.01$ *vs*. HFD. ND, normal diet; HFD, high-fat diet; Nit, nitazoxanide; Ato, atorvastatin.

hyperlipidemia, as manifested by the representative photographs of serum from animals in each group and the analyzed lipid parameters including total cholesterol (TC), triglyceride (TG), HDL-C, and LDL-C in serum (Fig. 2D). There was no difference of serum AST and ALT levels among the groups (Fig. 2D).

HFD feeding markedly altered the morphology appearance of hamster livers. As shown in Fig. 3A, in contrast to the livers with normal size and reddish-brown color in ND-fed hamsters, the livers of HFD-fed hamsters became swollen and pale in color; nitazoxanide treatment tended to restore the liver color and size. The body weight of HFD-fed hamsters decreased compared with that of ND (normal diet)-fed hamsters at the end of experiment, nitazoxanide treatment had no effect but atorvastatin (1.2 mg/kg/day) treatment further reduced the body weight of HFD-fed hamsters (Fig. 3B). Compared with ND, HFD feeding induced significant increases of liver weight and liver weight index (liver weight/body weight) of hamsters, and the increases were inhibited by nitazoxanide and atorvastatin treatments (Fig. 3B). Nitazoxanide and atorvastatin treatments reduced the increased liver TC level induced by HFD in hamsters (Fig. 3C). Although there was a statistical difference of liver TG level between HFD-fed and ND-fed hamsters, the extent of the liver TG increase in HFD-fed hamsters was slight and was reduced by nitazoxanide (200 mg/kg/day) treatment (Fig. 3C).

The livers of HFD-fed hamsters showed remarkable histopathologic changes. As shown by the hematoxylin/eosin (H&E)-stained liver paraffin sections in Fig. 3D, there existed apparent hydropic degeneration of hepatocytes and clustered Kupffer cells with size enlargement in livers of HFD-fed hamsters. Nitazoxanide treatment significantly improved these pathological features induced by HFD feeding. However, although atorvastatin (1.2 mg/kg/day) treatment corrected HFD-induced alteration of lipid profile, it did not improve HFD-induced liver histopathologic changes. The further oil red O staining displayed clusted lipid-laden Kupffer cells (foamy cells) in the liver sections from HFD and HFD plus Ato groups; however, no such features were detected in the liver sections from nitazoxanide treatment groups (Fig. 3E).

We further examined the protein expression and activity of AMPK and ACC in liver tissues, since AMPK activation and ACC inhibition by nitazoxanide and tizoxanide treatments had been demonstrated in HepG2 cells *in vitro* (Fig. 1E and F). As shown in Fig. 4A, the protein levels of AMPK and phosphorylated AMPK in livers of HFD-fed hamsters were lower relative to those of ND-fed hamsters, and nitazoxanide (100 and 200 mg/kg/day) treatment significantly increased the reduced AMPK and phosphorylated AMPK protein levels. Atorvastatin (1.2 mg/kg/day) treatment had no effect on the protein expression and activity of

AMPK in livers of HFD-fed hamsters. Accordingly, nitazoxanide (100 and 200 mg/kg/day) treatment increased the phosphorylation of ACC in livers from HFD-fed hamsters (Fig. 4B). These results indicate that nitazoxanide- and tizoxanide-induced AMPK activation *in vitro* could be recapitulated *in vivo*.

HFD feeding induced renal lipid accumulation[42] and renal injury[43,44]. In the present HFD-fed hamster model, we further detected the renal lipid accumulation. As shown in Supporting Information Fig. S10A, HFD feeding induced increase of kidney weight index (kidney weight/body weight) which was further increased by atorvastatin (1.2 mg/kg/day) treatment. H&E staining showed no significant histopathological change of kidneys in each group (Fig. S10B). However, oil red O staining results show significant renal lipid accumulation in HFD-fed hamsters, especially in glomerulus parts (Fig. S10C). The HFD-induced renal lipid accumulation was significantly attenuated by nitazoxanide and atorvastatin treatments (Fig. S10D). We established the relationship between the serum TC and TG with the oil red O staining

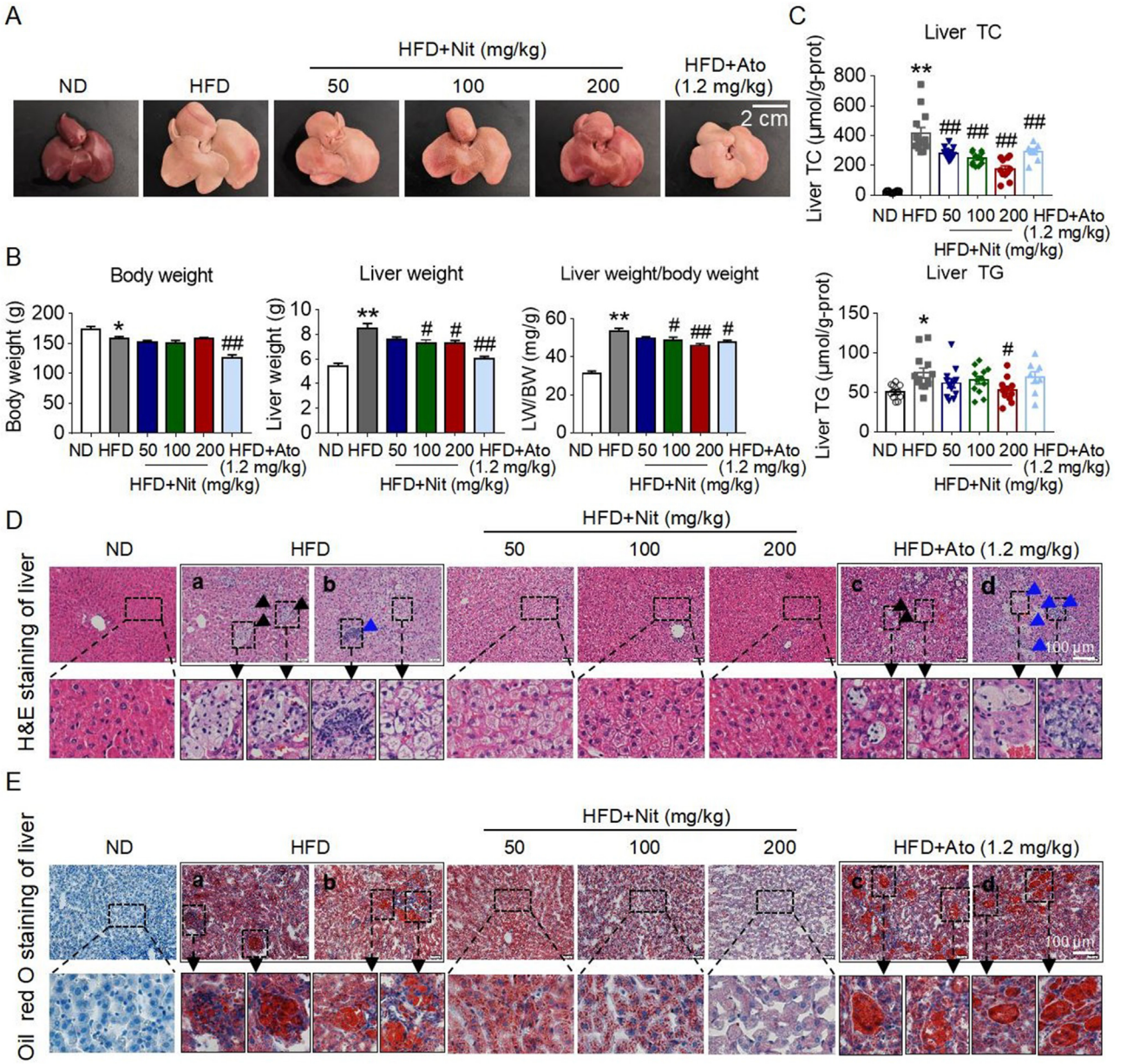

Figure 3 Gavage administration of nitazoxanide prevents HFD feeding-induced liver histopathology in hamsters. (A) The representative images of hamster livers from different groups. It was apparent that the liver from HFD group was swollen and pale in color. (B) The body weight, liver weight, and liver weight/body weight of hamsters from different groups. (C) The total cholesterol and triglyceride content of livers. TC, total cholesterol; TG, triglyceride. (D) Hematoxylin and eosin (H&E) staining of hamster livers from different groups. The framed area was enlarged. (E) Oil red O staining of hamster livers from different groups. The framed area was enlarged. Data are presented as mean ± SEM; n = 10, 13, 12, 12, 11, and 9 in ND, HFD, HFD + Nit (50 mg/kg), HFD + Nit (100 mg/kg), HFD + Nit (200 mg/kg), and HFD + Ato (1.2 mg/kg) groups, respectively. Statistical analysis was performed with one-way ANOVA. $^{*}P < 0.05$, $^{**}P < 0.01$ *vs*. ND. $^{\#}P < 0.05$, $^{\#\#}P < 0.01$ *vs*. HFD. ND, normal diet; HFD, high-fat diet; Nit, nitazoxanide; Ato, atorvastatin.

ratio of kidney sections in all animals in this batch of experiment. Results show that there existed a positive correlation between the serum TC and TG with oil red O staining ratio of kidneys (Supporting Information Fig. S11), indicating that HFD-induced renal lipid accumulation might be due to the increased serum lipids, nitazoxanide and atorvastatin treatment reduced the increased serum lipids, then subsequently diminished the renal lipid accumulation in hamsters.

3.4. *Gavage administration of nitazoxanide reverses high-fat diet (HFD)-induced hyperlipidemia and hepatic steatosis in hamsters*

Since nitazoxanide prevented HFD-induced hyperlipidemia and hepatic steatosis in hamsters, we wondered whether nitazoxanide treatment could reverse the pre-existing hyperlipidemia and hepatic steatosis in hamster model. To this end, firstly, we established the hyperlipidemia and hepatic steatosis model in hamsters fed with HFD for 25 days (Supporting Information Fig. S12A). Compared with ND, HFD feeding for 25 days showed no significant effect on the body weight of animals (Fig. S12B), but led to significant increases of liver weight and liver cholesterol content, and the liver color of HFD-fed animals became pale (Fig. S12C and S12D). Histological H&E staining showed that the hepatic cells of HFD-fed animals became hydropic degeneration, manifesting with cell swelling and edema (Fig. S12E). Oil red O staining shows increased lipid deposition in livers of HFD-fed animals (Fig. S12E).

It was very interesting that, although there was no difference of the body weight between ND- and HFD-fed hamsters, the weight and adipocyte size of perirenal white adipose tissue (prWAT) and epididymal white adipose tissue (eWAT) were increased in HFD-fed group (25 days) (Fig. S12F and S12G). HFD-feeding (25 days) also increased the weight of interscapular brown adipose tissue (iBAT) (Fig. S12H). Different from the clear and faint yellow appearance of serum from ND-fed hamsters, the serum from HFD-fed hamsters was milk-like (Fig. S12I). Quantitative results show that HFD-feeding (25 days) induced increases of serum TC, TG, LDL-C and HDL-C content in hamsters (Fig. S12J). Meanwhile, HFD-feeding (25 days) induced renal lipid accumulation (Supporting Information Fig. S13). Taken together, the hyperlipidemia and hepatic steatosis model was successfully established in hamsters fed with HFD for 25 days.

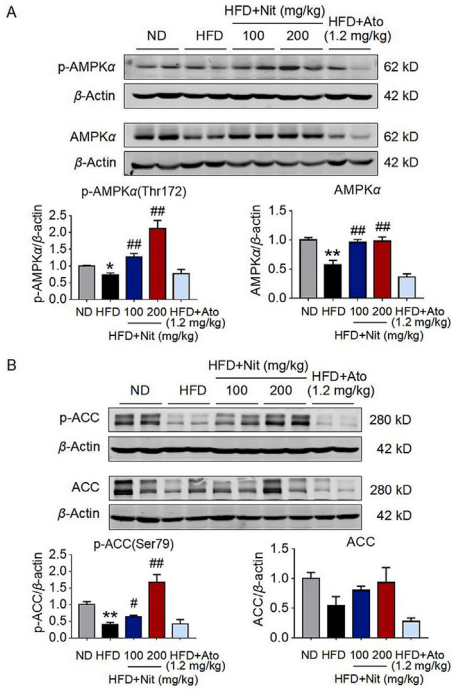

Figure 4 Gavage administration of nitazoxanide reverses HFD feeding-induced decreases of AMPK, phosphorylated AMPK and phosphorylate ACC protein levels in livers of hamsters. Data were presented as mean ± SEM; $n = 10$ in each group. Statistical analysis was performed with one-way ANOVA. $^{*}P < 0.05$, $^{**}P < 0.01$ *vs.* ND; $^{\#}P < 0.05$, $^{\#\#}P < 0.01$ *vs.* HFD. ND, normal diet; HFD, high-fat diet.

After confirming the model establishment, the remaining hamsters fed with HFD were randomly divided into two groups, HFD and HFD plus nitazoxanide groups. The hamsters were gavaged with solvent (control) or nitazoxanide (100 mg/kg/day, i.g.) respectively for further 25 days (Fig. 5A). The representative photographs of livers from each group were shown in Fig. 5B. The liver weight and liver weight index (LW/BW, liver weight/body weight) of HFD-fed hamsters were significantly higher than those of ND-fed hamsters, and nitazoxanide treatment significantly reduced the HFD-induced increase of liver weight and LW/BW (Fig. 5C). Nitazoxanide (100 mg/kg/day, i.g.) treatment reduced the HFD-induced increase of liver TC and TG content (Fig. 5D), improved HFD-induced hydropic degeneration of hepatic cells (Fig. 5E), and alleviated HFD-induced liver lipid deposit (Fig. 5F). Moreover, nitazoxanide (100 mg/kg/day, i.g.) treatment significantly increased the protein expression and activity of AMPK in livers from HFD-fed hamsters (Fig. 5G). The representative photographs of serum from hamsters in each group and the analyzed serum lipid parameters showed that nitazoxanide treatment reduced the increases of serum TC, TG, HDL-C, and LDL-C in HFD-fed hamsters (Fig. 5H and I).

Additionally, we further measured the weight and adipocyte size of perirenal white adipose tissue (prWAT) and epididymal white adipose tissue (eWAT) of hamsters in each group. Nitazoxanide treatment significantly reduced the increased weight and adipocyte size of prWAT and eWAT in HFD-fed hamsters (Supporting Information Fig. S14A−S14D), but showed no effect on the weight of interscapular brown adipose tissue (iBAT) (Fig. S14E). Nitazoxanide treatment did not significantly affect kidney weight index (kidney weight/body weight) (Supporting Information Fig. S15A) and kidney tissue histology detected by H&E staining (Fig. S15B), but reversed HFD-induced renal lipid accumulation as evaluated by oil red O staining assay (Fig. S15C and S15D). In this batch of experiment, the serum TC and TG levels were positive correlated to the oil red O staining ratio of kidney tissue sections in all animals (Fig. S15E).

3.5. *Gavage administration of nitazoxanide prevents high-fat diet (HFD)-induced hepatic steatosis in C57BL/6J mice*

In addition to using hamster model, we further used C57BL/6J mice fed with HFD for 16 weeks to induce hepatic steatosis. HFD or HFD plus nitazoxanide treatment for 16 weeks showed no significant effect on the morphological appearance of livers (Fig. 6A). Compared with the mice fed with ND, the body weight and liver weight of mice fed with HFD or HFD plus nitazoxanide increased (Fig. 6B). There was no statistical difference of liver weight index (liver weight/body weight) among the groups (Fig. 6B), indicating that the increased liver weight of mice fed

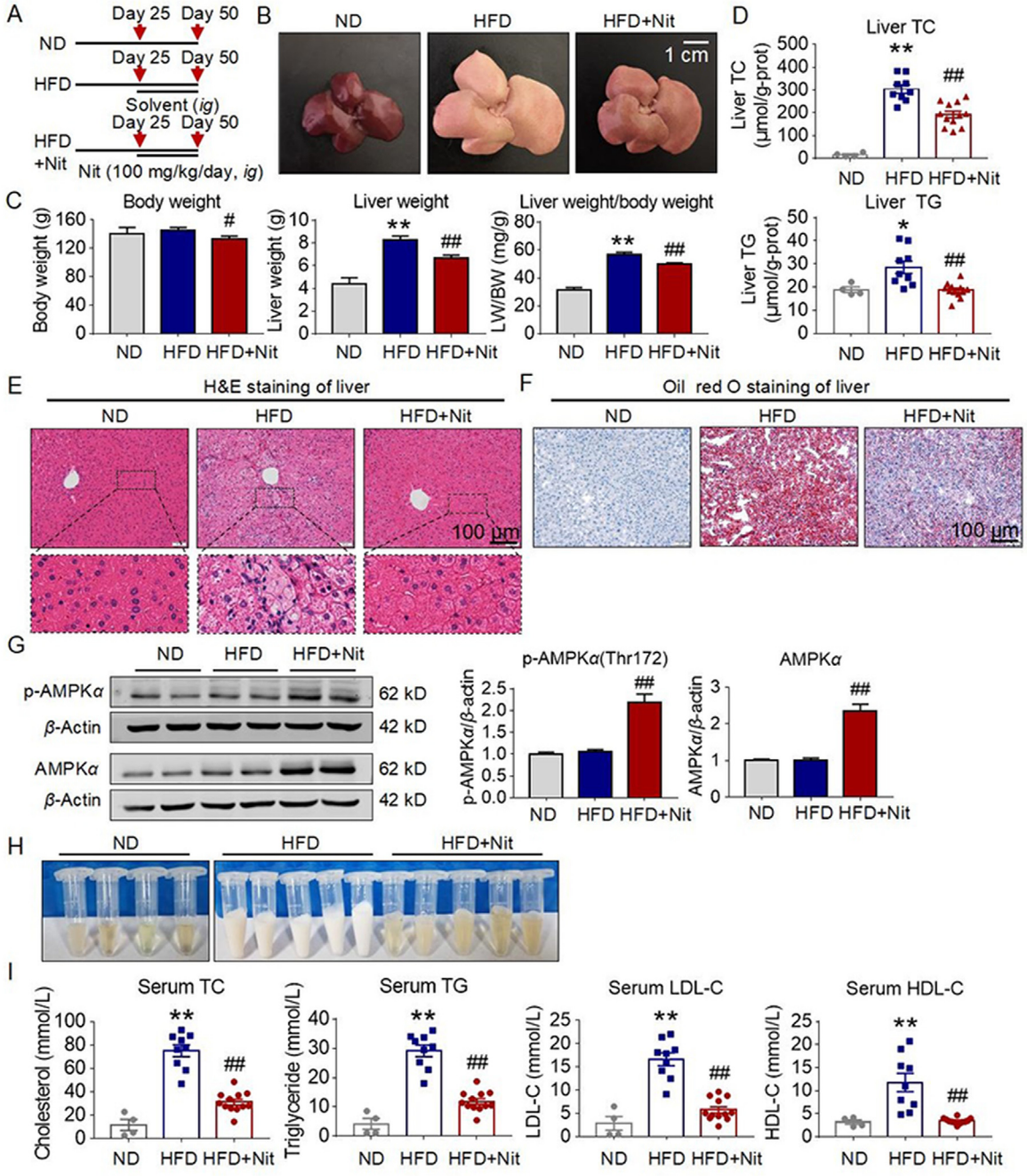

Figure 5 Gavage administration of nitazoxanide rescues HFD-induced hyperlipidemia and hepatic steatosis in hamsters. (A) Schematic illustration of the experiment design. (B) The representative images of livers. (C) The analyzed data of body weight, liver weight and liver weight/body weight (LW/BW). (D) The analyzed data of total cholesterol (TC) and triglyceride (TG) content in liver tissues. (E, F) The representative images of H&E and oil red O staining of livers. (G) Nitazoxanide increased phosphorylated AMPK and AMPK protein level in livers from HFD-fed hamsters. (H, I) Nitazoxanide reversed HFD-induced increase of serum cholesterol (TG), triglyceride (TC), LDL-C and HDL-C in hamsters. The serum images are shown in (H) and the quantitative data of serum TC, TG, LDL-C and HDL-C are shown in (I). Data are presented as mean ± SEM; $n = 4$, 9, and 12 in ND, HFD, and HFD + Nit groups, respectively. Statistical analysis was performed with one-way ANOVA. $^{*}P < 0.05$, $^{**}P < 0.01$ *vs*. ND; $^{\#\#}P < 0.01$ *vs*. HFD. ND, normal diet; HFD, high-fat diet; Nit, nitazoxanide; TC, total cholesterol; TG, triglyceride. HDL-C, high density lipoprotein cholesterol; LDL-C, high density lipoprotein cholesterol.

with HFD or HFD plus nitazoxanide was due to the increased body weight. However, the representative images of H&E-stained liver paraffin sections showed significant macrovesicular steatosis in livers of HFD-fed mice, and nitazoxanide treatment significantly improved the pathological properties (Fig. 6C). H&E staining is an indirect method for determining of lipid accumulation because lipid droplets in the tissues are dissolved by solvent during the specimen preparation. We further used the oil red O staining to validate the presence of large lipid deposits in livers of HFD-fed mice and the therapeutic effect of nitazoxanide treatment

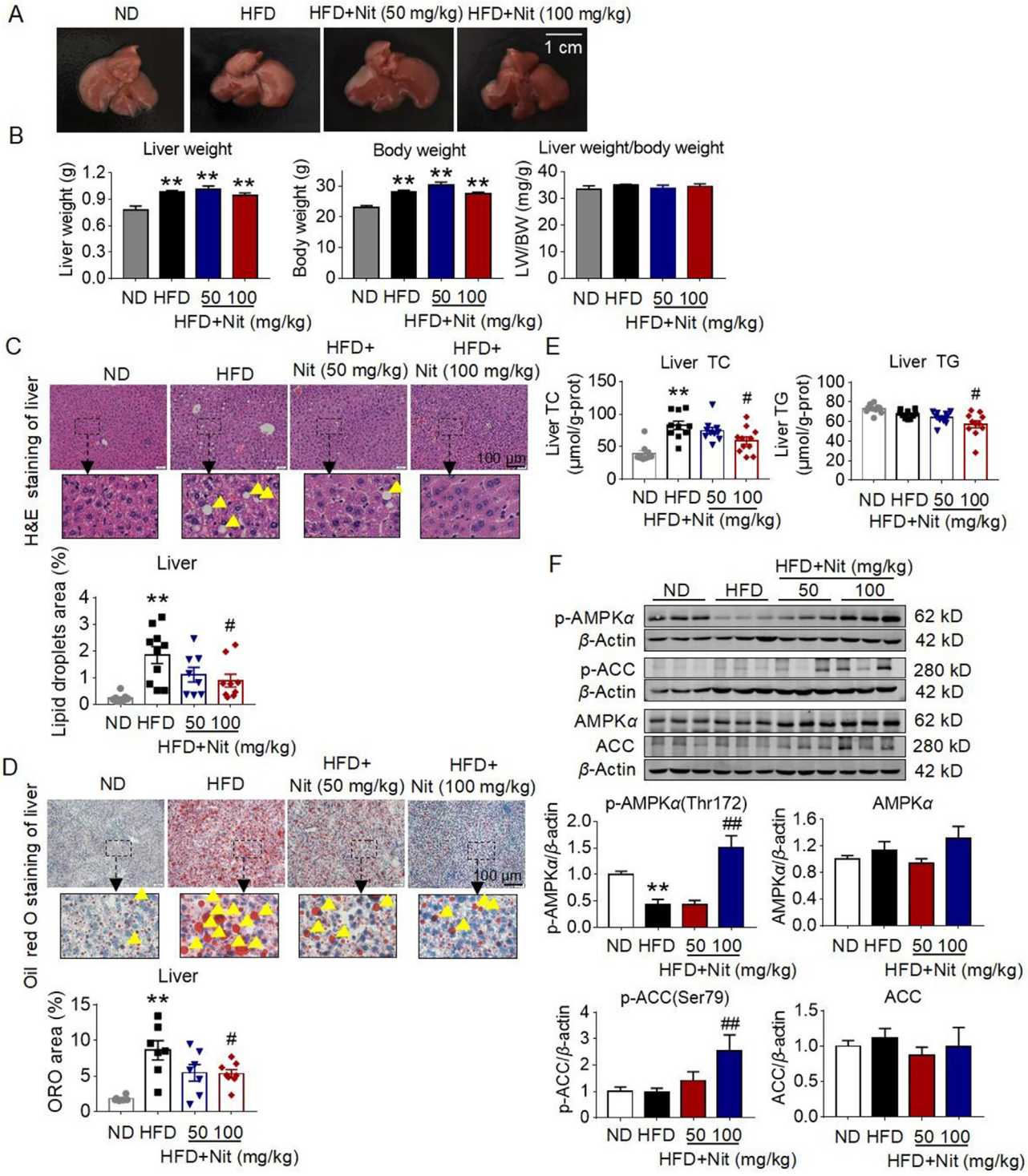

Figure 6 Gavage administration of nitazoxanide prevents HFD-induced hepatic steatosis in C57BL/6J mice. (A) The representative images of livers. (B) The analyzed data of body weight, liver weight, and liver weight/body weight (LW/BW). (C) The representative images of hematoxylin/eosin (H&E)-stained liver paraffin sections and the analyzed data of lipid deposits. (D) The representative images of oil red O staining of livers and the analyzed data of lipid deposits. (E) The analyzed data of TC and TG content in liver tissues. TC, total cholesterol; TG, triglyceride. (F) Nitazoxanide (100 mg/kg) increased phosphorylated AMPK and phosphorylated ACC protein level in livers. Data were presented as mean ± SEM; $n = 10$, 10, 10, and 11 in ND, HFD, HFD + Nit (50 mg/kg), HFD + Nit (100 mg/kg) groups, respectively. Statistical analysis was performed with one-way ANOVA. $^{**}P < 0.01$ *vs*. ND; $^{\#}P < 0.05$, $^{\#\#}P < 0.01$ *vs*. HFD. Nit, nitazoxanide.

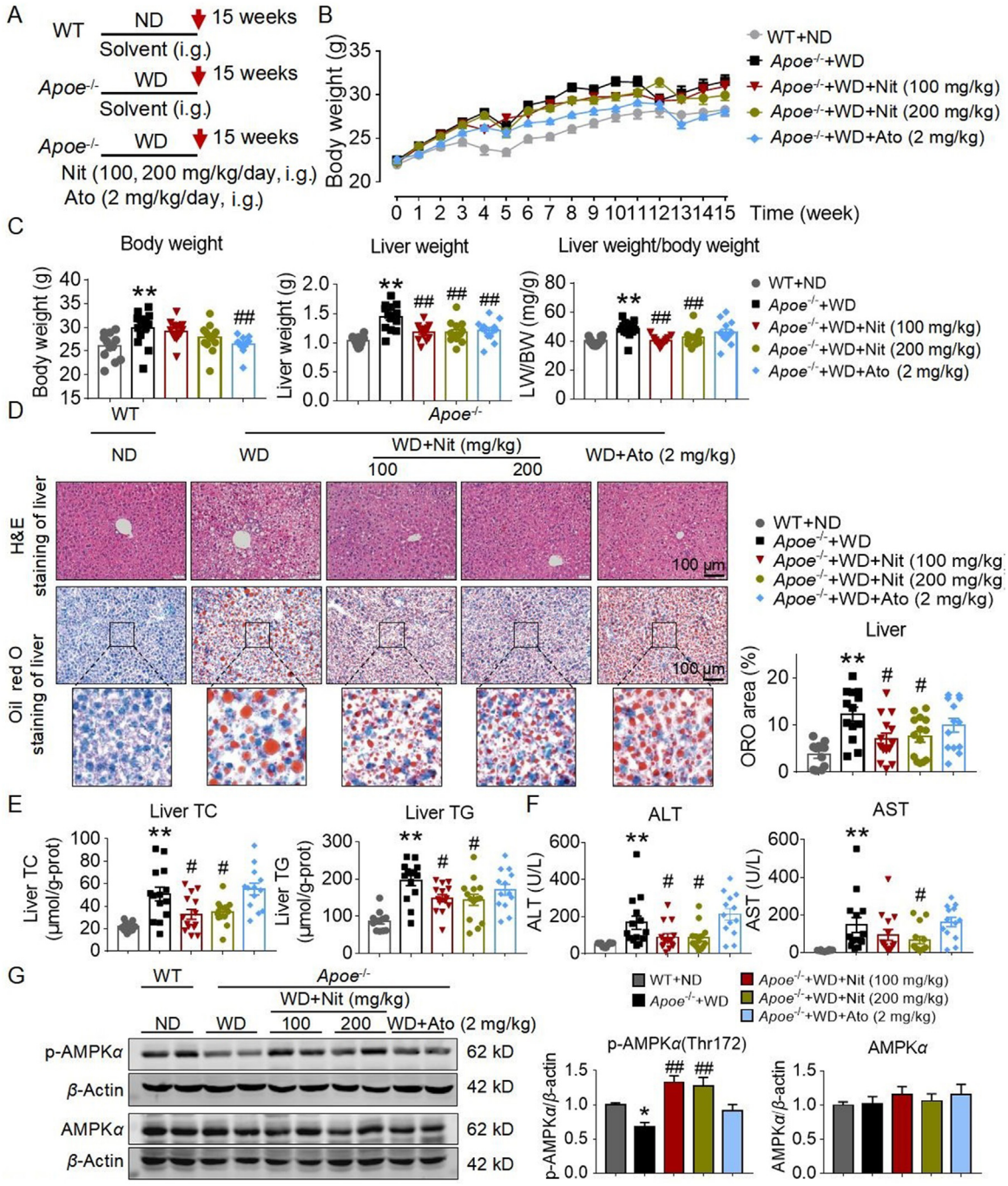

Figure 7 Gavage administration of nitazoxanide prevents western diet (WD) feeding-induced hepatic steatosis in *Apoe*$^{-/-}$ mice. (A) Schematic illustration of the experiment design. (B) The time course of body weight. (C) The analyzed data of body weight, liver weight, and liver weight/body weight (LW/BW). (D) The representative images of H&E and oil red O staining of livers. The framed area are enlarged. The analyzed data of oil red O staining was calculated by the area of positive red staining divided by the total area of sections. (E) The analyzed data of TC and TG content in liver tissues. TC, total cholesterol; TG, triglyceride. (F) The serum transaminase level of *Apoe*$^{-/-}$ mice. ALT, aspartate aminotransferase; AST, alanine aminotransferase. (G) Nitazoxanide increased phosphorylated AMPK protein level in livers of *Apoe*$^{-/-}$ mice. Data were presented as mean ± SEM; n = 12, 14, 14, 14, and 13 in WT + ND, *Apoe*$^{-/-}$+WD, *Apoe*$^{-/-}$+WD + Nit (100 mg/kg), *Apoe*$^{-/-}$+WD + Nit (200 mg/kg), *Apoe*$^{-/-}$+WD + Ato (2 mg/kg) groups, respectively. Statistical analysis was performed with one-way ANOVA. $^{*}P < 0.05$, $^{**}P < 0.01$ *vs.* WT + ND; $^{\#}P < 0.05$, $^{\#\#}P < 0.01$ *vs.* *Apoe*$^{-/-}$+WD.

(Fig. 6D). The results of liver TC and TG quantification show that HFD induced significant increase of TC which was inhibited by nitazoxanide (100 mg/kg/day) treatment; HFD had no effect on liver TG content but nitazoxanide treatment (100 mg/kg/day) further decreased it (Fig. 6E). Finally, the AMPK and ACC activities in liver tissues were examined. As shown in Fig. 6F, the AMPK activity of liver tissues from HFD-fed mice decreased and was significantly restored by nitazoxanide (100 mg/kg/day) treatment. Nitazoxanide (100 mg/kg/day) treatment increased phosphorylation of ACC in liver tissue from HFD-fed mice (Fig. 6F). It was noteworthy that HFD for 16 weeks had no significant effect on serum levels of TC, TG, HDL-C, and LDL-C in C57BL/6J mice (Supporting Information Fig. S16A and S16B); parallel, no renal lipid accumulation was detected by oil red O staining in the animals (Fig. S16C).

3.6. *Gavage administration of nitazoxa nide improves western diet (WD)-induced hepatic steatosis in Apoe$^{-/-}$ mice*

Western diet induces hepatic steatosis in *Apoe*$^{-/-}$ mice[45,46]. We fed *Apoe*$^{-/-}$ mice for 15 weeks to establish the hepatic steatosis model. In the experiment, nitazoxanide was gavaged to the mice at the doses of 100 and 200 mg/kg/day and atorvastatin at 2 mg/kg/day as the positive drug (Fig. 7A). The time course of body weight during the 15 weeks was shown in Fig. 7B. Compared with the wild type (WT) animals fed with ND, *Apoe*$^{-/-}$ mice fed with WD showed increased body weight, liver weight, and liver weight/body weight (LW/BW), which was inhibited by nitazoxanide treatment (100 and 200 mg/kg/day, Fig. 7C). H&E and oil red O staining results showed that there existed significant lipid deposits in livers of WD-fed *Apoe*$^{-/-}$ mice which were mitigated by nitazoxanide treatment (Fig. 7D). The increased liver TC, TG and serum ALT, AST in WD-fed *Apoe*$^{-/-}$ mice were reduced by nitazoxanide treatment (Fig. 7E and F). The AMPK activity of liver tissues from WD-fed *Apoe*$^{-/-}$ mice decreased and was significantly restored by nitazoxanide treatment (Fig. 7G). Additionally, nitazoxanide treatment increased LC3-II protein level and LC3-II/LC3-I ratio in liver tissues of WD-fed *Apoe*$^{-/-}$ mice (Supporting Information Fig. S17), consistent with the results that both nitazoxanide and tizoxanide induced autophagy in HepG2 cells *in vitro* (Fig. S5). However, atorvastatin at the dose (2 mg/kg/day) equivalent to the recommended in clinic showed no effect on the increased liver lipid deposit, liver TC and TG and serum ALT and AST, and no effect on autophagy and the impaired AMPK activity in liver tissues except that it reduced the body weight and liver weight of WD-fed *Apoe*$^{-/-}$ mice (Fig. 7C).

Nitazoxanide treatment reduced the increased kidney weight but had no significant effect on the increased kidney weight index (kidney weight/body weight) in WD-fed *Apoe*$^{-/-}$ mice (Supporting Information Fig. S18A). Atorvastatin treatment reduced the increased kidney weight and kidney weight index in WD-fed *Apoe*$^{-/-}$ mice (Fig. S18A). H&E staining results showed no significant difference of histology among the groups (Fig. S18B); however, Oil red O staining results displayed significant lipid accumulation in renal tubules of WD-fed *Apoe*$^{-/-}$ mice (Fig. S18C), which was different from that in glomerulus of HFD-fed hamsters (Fig. S10, S13 and S15). Nitazoxanide treatment significantly ameliorated the lipid accumulation in renal tubules of WD-fed *Apoe*$^{-/-}$ mice (Fig. S18C and S18D). WD feeding increased serum levels of TC, TG and LDL-C, but decreased HDL-C, and nitazoxanide treatment reduced the increased serum TC and further reduced the decreased HDL-C in *Apoe*$^{-/-}$ mice (Fig. S19). Interestingly, in contrast to that in hamsters, there was no a correlationship between the serum TC and TG levels and the oil red O staining ratio of kidney tissue sections in WD-fed *Apoe*$^{-/-}$ mice model (Fig. S20).

In order to confirm the above results, we further performed another experiment with WD-feeding for 21 weeks in *Apoe*$^{-/-}$ mice. The experiment design was shown in Supporting Information Fig. S21A. The time course of body weight is shown in Fig. S21B. *Apoe*$^{-/-}$ mice fed with WD (21 weeks) displayed increased liver weight/body weight, liver TC and TG, and liver lipid deposit, which were reduced by nitazoxanide treatment (100 mg/kg/day, i.g.) (Fig. S21C−S21F). *Apoe*$^{-/-}$ mice fed with WD (21 weeks) also showed decreased AMPK activity in liver tissues which was restored by nitazoxanide treatment (100 mg/kg/day, i.g.) (Supporting Information Fig. S22A and S22B). Meanwhile, we further detected the autophagic parameters including LC3-I, LC3-II, and SQSTM1/P62 protein levels and LC3-II/LC3-I ratio. As shown in Fig. S22C and S22D, the protein expression of LC3-II and P62 and the LC3-II/LC3-I ratio were significantly decreased in liver tissues from WD-fed *Apoe*$^{-/-}$ mice and the decreases were reversed by nitazoxanide treatment (100 mg/kg/day, i.g.).

4. Discussion

Lipid metabolism disorders encompasses a spectrum of diseases including hyperlipidemia, atherosclerosis, and hepatic steatosis which are strongly associated with the occurrence of diabetes mellitus and cardiovascular events. In view of the role of mitochondrial uncoupling in the regulation of metabolism[47−50], the small chemical mitochondrial uncouplers have been strongly attractive for drug development to improve metabolic diseases[14,35,49,51−54]. However, the biggest problem for the development of mitochondrial uncouplers as clinical drugs is their narrow therapeutic window between efficacy and toxicity. The most typical example is 2,4-dinitrophenol (DNP) which was clinically used as a weight loss drug in the 1930s but withdrawn from the market in 1938 due to its toxicities. In order to avoid the risk of infeasibility of mitochondrial uncoupler candidates when used in clinic, based on the mitochondrial uncoupling mechanism, we aimed to find the candidates with uncoupling effect from the existing drugs and rediscover their new therapeutic application for metabolic disorders. Here, we found that anthelmintics drug nitazoxanide and its metabolite tizoxanide induced mitochondrial uncoupling and activated AMPK in HepG2 cells *in vitro*, and proved that nitazoxanide protected against the experimental hyperlipidemia and hepatic steatosis in hamsters and mice *in vivo*. The potential mechanisms of nitazoxanide action were summarized in Fig. 8. Nitazoxanide has a good safety profile at the doses used in the present study, which have been evidenced in the previous clinical trials[40,41]. Therefore, repurposing nitazoxanide as a novel drug for hyperlipidemia and hepatic steatosis treatment is promising.

The inspiration of this project originated from our previous studies about the small molecule mitochondrial uncouplers[18−20,55−57] and the similar chemical structure shared by niclosamide and tizoxanide, nitazoxanide (Fig. S1). Nitazoxanide was synthesized on the scaffold of niclosamide in replacing one benzene ring, a 6-membered ring heterocycle, by a nitrothiazole, a 5-membered ring heterocycle[13]. The above information indicates that nitazoxanide might have similar effect as niclosamide which has been reported to improve hepatic steatosis in mice[14]. The disadvantage of niclosamide is its poor solubility and poor oral bioavailability, whereas nitazoxanide has good bioavailability and safety profile. We speculated that nitazoxanide

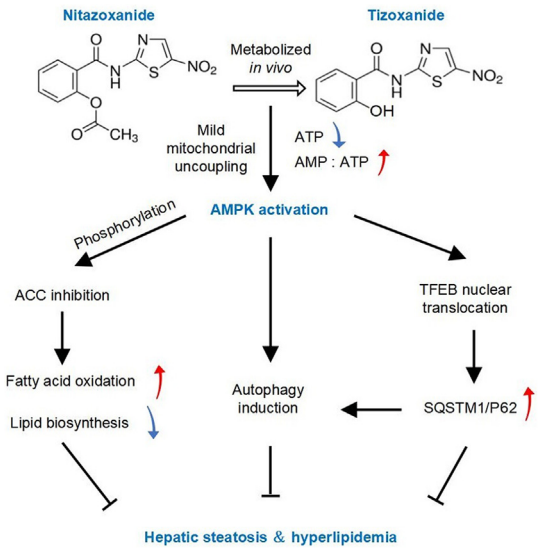

Figure 8 A schematic diagram summarizing the potential mechanisms that nitazoxanide protects against experimental hyperlipidemia and hepatic steatosis.

would have a superior effect of improving hyperlipidemia and hepatic steatosis *in vivo*, and the present data proved our hypothesis indeed.

Nitazoxanide is rapidly hydrolyzed to tizoxanide after entering systemic circulation, so in the pharmacokinetics study of nitazoxanide, the plasma concentration of tizoxanide was measured. The C_{max} of tizoxanide in healthy volunteers following single or multiple-dose oral administration of nitazoxanide 500 mg tablets was around 9 μg/mL[58], so we thought that the concentration of tizoxanide used in the present *in vitro* experiments could match with that *in vivo*. Although only tizoxanide not nitazoxanide is detected in plasma after nitazoxanide absorption, we examined the effects of both nitazoxanide and tizoxanide *in vitro* and results showed that they have similar efficacy and potency.

Both elevated blood lipids and liver lipids belong to lipid metabolism disorders, but their relationship is correlative, not reciprocally causal. Presently, there is no consensus of application of the lipid lowering agents for hepatic steatosis treatment. The typical statins used in patients with nonalcoholic fatty liver disease (NAFLD) and nonalcoholic steatohepatitis (NASH) are due to decreasing the risk of cardiovascular events rather than improving liver pathology[59]. On the other hand, vitamin E and pioglitazone recommended for NASH treatment don't belong to lipid lowering agents[59]. It was even reported that the approaches to reduce hepatic steatosis elevated blood lipids[9,10]. Therefore, it will be ideal to develop drugs simultaneous improving both hyperlipidemia and hepatic steatosis. In the present HFD-fed hamster model, we measured the effect of nitazoxanide on hyperlipidemia and hepatic steatosis with atorvastatin as a positive drug. We found that nitazoxanide had equivalent effect of lowering blood lipids as atorvastatin; however, nitazoxanide treatment significantly improved the liver pathological changes including hepatocyte hydropic degeneration and the appearance of many clusted lipid-laden Kupffer cells (foamy cells) in HFD-fed hamsters whereas the improvement cannot be detected in atorvastatin treated HFD-fed hamsters, though atorvastatin treatment reduced the liver TC and TG. In the present WD-fed *Apoe*$^{-/-}$ mice model, atorvastatin (2 mg/kg/day) treatment showed no effect on the increased liver lipid deposit, liver TC and TG and serum ALT and AST, and no effect on autophagy and the impaired AMPK activity in liver tissues of WD-fed *Apoe*$^{-/-}$ mice. In fact, the animals had response to atorvastatin at this dose because atorvastatin (2 mg/kg/day) treatment reduced the body weight of WD-fed *Apoe*$^{-/-}$ mice. Wu et al.[60] reported that atorvastatin exacerbated hepatic steatosis, inflammation and fibrosis in *Apoe*$^{-/-}$ mice fed with western diet and injected with casein. In aspect of improving liver histopathology, nitazoxanide was markedly superior to statins.

In the present study, we used two animal species, hamsters and mice. Although the two species of animals were fed with the similar HFD or WD for the similar duration, they showed different pathological features. The most typical difference lies that, in both C57BL/6J mice fed with HFD and *Apoe*$^{-/-}$ mice fed with WD, their livers exhibited typical lipid droplets; however, in hamsters fed with HFD, their livers mainly presented hepatocyte hydropic degeneration and clusted lipid-laden Kupffer cells (foamy cells) without typical lipid droplets detected. On the other hand, HFD feeding induced renal lipid accumulation in glomerulus in hamsters whereas WD feeding induced lipid accumulation in renal tubules in *Apoe*$^{-/-}$ mice. Furthermore, in HFD-fed hamster model, there existed a positive correlationship between the serum TC and TG levels with oil red O staining ratio of kidney tissue sections, but no correlationship in WD-fed *Apoe*$^{-/-}$ mice model. These findings imply that the pathological mechanisms in different species might be distinct even under the same pathological stimulation.

In the present study, we performed two batches of experiments by using hamsters and *Apoe*$^{-/-}$ mice respectively. In the two experiments with HFD-fed hamsters, we fed the animals with the same HFD for the same duration, the features of liver pathological changes were similar but the extent was not identical. Compared with the first experiment (Figs. 2−4), the degree of liver pathological changes was relatively slight, and AMPK activity and protein expression did not decrease in the second batch of experiment (Fig. 5). However, in both batches of experiments, nitazoxanide treatment showed significant effect of activating AMPK in liver tissues of hamsters. In the two experiments with WD-fed *Apoe*$^{-/-}$ mice, we fed the animals with the same WD for different duration, 15 and 21 weeks. It was apparently that the longer duration of WD feeding, the more severe of lipid deposit and impairment of AMPK activity in livers. The LC3-II and P62 protein expressions in livers were not changed in *Apoe*$^{-/-}$ mice fed with WD for 15 weeks, but significantly decreased in *Apoe*$^{-/-}$ mice fed with WD for 21 weeks. To our knowledge, it was the first finding that P62 protein expression almost disappeared in livers of *Apoe*$^{-/-}$ mice fed with WD, and more amazingly, nitazoxanide treatment completely restored the down-regulated P62 protein expression (Fig. S22C and S22D). SQSTM1/P62 itself has been reported to protect liver from lipotoxicity and fibrosis[61,62], therefore, up-regulating SQSTM1/P62 expression might be at least as one of the mechanisms contributing to the protective effect of nitazoxanide against hepatic steatosis.

For the experiments to determine the effect of nitazoxanide on the pre-existing hyperlipidemia and hepatic steatosis in hamsters, it will be ideal to use a noninvasive approach to determine the liver pathological changes of each animal before the drug treatment. However, the specificity and sensitivity of the present noninvasive methods are limited. Even in the process of diagnosing human hepatic steatosis, the diagnostic accuracy of imaging methods such as ultrasound and CT requires that the lipid droplet deposition in the livers reaches more than 30%[63]. Therefore, we designed the experiments in two steps. Firstly, five hamsters were sampled randomly from the ND and HFD-fed groups respectively on Day 25 to determine the establishment of

hyperlipidemia and hepatic steatosis model (Fig. S12A); then, the remaining HFD-fed hamsters were randomly divided into HFD and HFD plus nitazoxanide groups for the subsequent experiments to Day 50 (Fig. 5A). This experiment design ensured the parallel between each group and avoided the interference factors.

Since nitazoxanide has showed excellent effect of improving lipid metabolic disorders in the experimental models, our most concern is the safety of nitazoxanide when used for clinical therapy. The acute and subchronic toxicology of nitazoxanide in animals had proved that nitazoxanide was of safety. Nitazoxanide was negative in the Ames Salmonella assay. The acute oral LD_{50} values of nitazoxanide were greater than 10 g/kg in rats, dogs and cats[64]. In a randomized controlled clinical trial, nitazoxanide monotherapy for 12 weeks followed by nitazoxanide plus peginterferon alpha-2a and ribavirin for 36 weeks was designed for chronic hepatitis C treatment, and nitazoxanide (500 mg) was given twice daily. Results showed that the combination of nitazoxanide did not increase adverse events compared with standard therapeutic (peginterferon alpha-2a and ribavirin for 48 weeks)[41]. In another pilot proof-of-concept clinical trial of nitazoxanide in treating chronic hepatitis B, nitazoxanide 500 mg tablets were administered orally twice daily up to 48 weeks and well tolerated[40]. Recently, the dose for repurposing nitazoxanide in SARS-CoV-2 treatment or chemoprophylaxis in human has been suggested to be 1200 mg QID, 1600 mg TID and 2900 mg BID in the fasted state and 700 mg QID, 900 mg TID and 1400 mg BID when given with food[65]. In the present study, the effective doses (50, 100, and 200 mg/kg/day) of nitazoxanide used in hamsters and mice *in vivo* were equivalent to the doses in human clinical trials, indicating that application of nitazoxanide for treating lipid metabolic disorders in clinic was feasible.

Although we focused on the protective effect of nitazoxanide against hyperlipidemia and hepatic steatosis, we also investigated the effect of nitazoxanide on HFD- or WD-induced renal lipid accumulation. We found that nitazoxanide treatment significantly ameliorated HFD-induced renal lipid accumulation in glomerulus in hamsters and WD-induced renal lipid accumulation in renal tubules in *Apoe*$^{-/-}$ mice. In view of the lipotoxicity in kidneys, our results indicate that nitazoxanide might also be protective against HFD-induced kidney injury.

5. Conclusions

Nitazoxanide and its active metabolite tizoxanide induce mild mitochondrial uncoupling and activate AMPK in hepatocytes, and gavage administration of nitazoxanide protects against experimental hyperlipidemia and hepatic steatosis in hamsters and mice. The present work suggests a promising translation for nitazoxanide to be used for hyperlipidemia and MAFLD in clinic.

Acknowledgments

This study was supported by the National Natural Science Foundation of China (Nos. 81773725 and 91739102).

Author contributions

Fengfeng Li, Man Jiang, Minghui Ma, Xuyang Chen, Yidan Zhang, Yixin Zhang, Yuanyuan Yu, Yunfeng Cui, Jiahui Chen and Hui Zhao conducted the experiments, data analysis and figure preparation. Zhijie Sun and Deli Dong provided the concept, designed the study and edited the manuscript. All authors have given approval to the final version of the manuscript.

Conflicts of interest

The authors declare no conflicts of interest.

Appendix A. Supporting information

Supporting data to this article can be found online at https://doi.org/10.1016/j.apsb.2021.09.009.

References

1. Eslam M, Newsome PN, Sarin SK, Anstee QM, Targher G, Romero-Gomez M, et al. A new definition for metabolic dysfunction-associated fatty liver disease: an international expert consensus statement. *J Hepatol* 2020;**73**:202–9.
2. Eslam M, Sanyal AJ, George J, International Consensus P. Mafld: a consensus-driven proposed nomenclature for metabolic associated fatty liver disease. *Gastroenterology* 2020;**158**:1999–2014.e1.
3. Machado MV, Cortez-Pinto H. Non-alcoholic fatty liver disease: what the clinician needs to know. *World J Gastroenterol* 2014;**20**:12956–80.
4. Weber C, Noels H. Atherosclerosis: current pathogenesis and therapeutic options. *Nat Med* 2011;**17**:1410–22.
5. Ouchi Y, Sasaki J, Arai H, Yokote K, Harada K, Katayama Y, et al. Ezetimibe lipid-lowering trial on prevention of atherosclerotic cardiovascular disease in 75 or older (ewtopia 75): a randomized, controlled trial. *Circulation* 2019;**140**:992–1003.
6. Vallejo-Vaz AJ, Robertson M, Catapano AL, Watts GF, Kastelein JJ, Packard CJ, et al. Low-density lipoprotein cholesterol lowering for the primary prevention of cardiovascular disease among men with primary elevations of low-density lipoprotein cholesterol levels of 190 mg/dL or above: analyses from the woscops (west of scotland coronary prevention study) 5-year randomized trial and 20-year observational follow-up. *Circulation* 2017;**136**:1878–91.
7. Hirata T, Tomita K, Kawai T, Yokoyama H, Shimada A, Kikuchi M, et al. Effect of telmisartan or losartan for treatment of nonalcoholic fatty liver disease: fatty liver protection trial by telmisartan or losartan study (fantasy). *Int J Endocrinol* 2013;**2013**:587140.
8. Zein CO, Yerian LM, Gogate P, Lopez R, Kirwan JP, Feldstein AE, et al. Pentoxifylline improves nonalcoholic steatohepatitis: a randomized placebo-controlled trial. *Hepatology* 2011;**54**:1610–9.
9. Goedeke L, Bates J, Vatner DF, Perry RJ, Wang T, Ramirez R, et al. Acetyl-CoA carboxylase inhibition reverses nafld and hepatic insulin resistance but promotes hypertriglyceridemia in rodents. *Hepatology* 2018;**68**:2197–211.
10. Kim CW, Addy C, Kusunoki J, Anderson NN, Deja S, Fu X, et al. Acetyl CoA carboxylase inhibition reduces hepatic steatosis but elevates plasma triglycerides in mice and humans: a bedside to bench investigation. *Cell Metab* 2017;**26**:394–406.e6.
11. Hussar DA. New drugs of 2003. *J Am Pharm Assoc (2003)* 2004;**44**:168–206. quiz 7-10.
12. Jasenosky LD, Cadena C, Mire CE, Borisevich V, Haridas V, Ranjbar S, et al. The FDA-approved oral drug nitazoxanide amplifies host antiviral responses and inhibits Ebola virus. *iScience* 2019;**19**:1279–90.
13. Rossignol JF. Nitazoxanide: a first-in-class broad-spectrum antiviral agent. *Antiviral Res* 2014;**110**:94–103.
14. Tao H, Zhang Y, Zeng X, Shulman GI, Jin S. Niclosamide ethanolamine-induced mild mitochondrial uncoupling improves diabetic symptoms in mice. *Nat Med* 2014;**20**:1263–9.

15. Percie du Sert N, Hurst V, Ahluwalia A, Alam S, Avey MT, Baker M, et al. The arrive guidelines 2.0: updated guidelines for reporting animal research. *PLoS Biol* 2020;**18**:e3000410.
16. Percie du Sert N, Ahluwalia A, Alam S, Avey MT, Baker M, Browne WJ, et al. Reporting animal research: explanation and elaboration for the arrive guidelines 2.0. *PLoS Biol* 2020;**18**:e3000411.
17. Zhao J, Gao JL, Zhu JX, Zhu HB, Peng X, Jiang M, et al. The different response of cardiomyocytes and cardiac fibroblasts to mitochondria inhibition and the underlying role of STAT3. *Basic Res Cardiol* 2019; **114**:12.
18. Xiao XL, Hu N, Zhang XZ, Jiang M, Chen C, Ma R, et al. Niclosamide inhibits vascular smooth muscle cell proliferation and migration and attenuates neointimal hyperplasia in injured rat carotid arteries. *Br J Pharmacol* 2018;**175**:1707−18.
19. Gao JL, Zhao J, Zhu HB, Peng X, Zhu JX, Ma MH, et al. Characterizations of mitochondrial uncoupling induced by chemical mitochondrial uncouplers in cardiomyocytes. *Free Radic Biol Med* 2018;**124**:288−98.
20. Zhang YQ, Shen X, Xiao XL, Liu MY, Li SL, Yan J, et al. Mitochondrial uncoupler carbonyl cyanide *m*-chlorophenylhydrazone induces vasorelaxation without involving K channel activation in smooth muscle cells of arteries. *Br J Pharmacol* 2016;**173**:3145−58.
21. Dashti N. The effect of low density lipoproteins, cholesterol, and 25-hydroxycholesterol on apolipoprotein B gene expression in HepG2 cells. *J Biol Chem* 1992;**267**:7160−9.
22. Ren G, Guo JH, Qian YZ, Kong WJ, Jiang JD. Berberine improves glucose and lipid metabolism in HepG2 cells through AMPKalpha1 activation. *Front Pharmacol* 2020;**11**:647.
23. Vendel Nielsen L, Krogager TP, Young C, Ferreri C, Chatgilialoglu C, Norregaard Jensen O, et al. Effects of elaidic acid on lipid metabolism in HepG2 cells, investigated by an integrated approach of lipidomics, transcriptomics and proteomics. *PLoS One* 2013;**8**:e74283.
24. Amireddy N, Puttapaka SN, Vinnakota RL, Ravuri HG, Thonda S, Kalivendi SV. The unintended mitochondrial uncoupling effects of the FDA-approved anti-helminth drug nitazoxanide mitigates experimental parkinsonism in mice. *J Biol Chem* 2017;**292**:15731−43.
25. Li Y, Chen Y. AMPK and autophagy. *Adv Exp Med Biol* 2019;**1206**: 85−108.
26. Kim SH, Kim G, Han DH, Lee M, Kim I, Kim B, et al. Ezetimibe ameliorates steatohepatitis *via* AMP activated protein kinase-TFEB-mediated activation of autophagy and NLRP3 inflammasome inhibition. *Autophagy* 2017;**13**:1767−81.
27. Park HS, Song JW, Park JH, Lim BK, Moon OS, Son HY, et al. TXNIP/VDUP1 attenuates steatohepatitis *via* autophagy and fatty acid oxidation. *Autophagy* 2020;**16**:1−16.
28. Lam KK, Zheng X, Forestieri R, Balgi AD, Nodwell M, Vollett S, et al. Nitazoxanide stimulates autophagy and inhibits mTORC1 signaling and intracellular proliferation of mycobacterium tuberculosis. *PLoS Pathog* 2012;**8**:e1002691.
29. Fan L, Qiu XX, Zhu ZY, Lv JL, Lu J, Mao F, et al. Nitazoxanide, an anti-parasitic drug, efficiently ameliorates learning and memory impairments in ad model mice. *Acta Pharmacol Sin* 2019;**40**:1279−91.
30. Bjørkøy G, Lamark T, Pankiv S, Øvervatn A, Brech A, Johansen T. Monitoring autophagic degradation of p62/SQSTM1. *Methods Enzymol* 2009;**452**:181−97.
31. Chen G, Xie W, Nah J, Sauvat A, Liu P, Pietrocola F, et al. 3,4-Dimethoxychalcone induces autophagy through activation of the transcription factors TFE3 and TFEB. *EMBO Mol Med* 2019;**11**:e10469.
32. Pan B, Li J, Parajuli N, Tian Z, Wu P, Lewno MT, et al. The calcineurin-TFEB-p62 pathway mediates the activation of cardiac macroautophagy by proteasomal malfunction. *Circ Res* 2020;**127**:502−18.
33. Alexopoulos SJ, Chen SY, Brandon AE, Salamoun JM, Byrne FL, Garcia CJ, et al. Mitochondrial uncoupler BAM15 reverses diet-induced obesity and insulin resistance in mice. *Nat Commun* 2020; **11**:2397.
34. Axelrod CL, King WT, Davuluri G, Noland RC, Hall J, Hull M, et al. BAM15-mediated mitochondrial uncoupling protects against obesity and improves glycemic control. *EMBO Mol Med* 2020;**12**:e12088.
35. Jian C, Fu J, Cheng X, Shen LJ, Ji YX, Wang X, et al. Low-dose sorafenib acts as a mitochondrial uncoupler and ameliorates nonalcoholic steatohepatitis. *Cell Metab* 2020;**31**:892−908.e11.
36. Ripani P, Delp J, Bode K, Delgado ME, Dietrich L, Betzler VM, et al. Thiazolides promote G1 cell cycle arrest in colorectal cancer cells by targeting the mitochondrial respiratory chain. *Oncogene* 2020;**39**: 2345−57.
37. Bhathena J, Kulamarva A, Martoni C, Urbanska AM, Malhotra M, Paul A, et al. Diet-induced metabolic hamster model of nonalcoholic fatty liver disease. *Diabetes Metab Syndr* 2011;**4**:195−203.
38. Bravo E, Cantafora A, Calcabrini A, Ortu GJCB, Biochemistry PPBC. Why prefer the golden syrian hamster (mesocricetus auratus) to the Wistar rat in experimental studies on plasma lipoprotein metabolism?. *Comp Biochem Physiol B Biochem Mol Biol* 1994;**107**:347−55.
39. Sullivan MP, Cerda JJ, Robbins FL, Burgin CW, Beatty RJ. The gerbil, hamster, and Guinea pig as rodent models for hyperlipidemia. *Lab Anim Sci* 1993;**43**:575−8.
40. Rossignol JF, Bréchot C. A pilot clinical trial of nitazoxanide in the treatment of chronic hepatitis B. *Hepatol Commun* 2019;**3**:744−7.
41. Rossignol JF, Elfert A, El-Gohary Y, Keeffe EB. Improved virologic response in chronic hepatitis C genotype 4 treated with nitazoxanide, peginterferon, and ribavirin. *Gastroenterology* 2009;**136**:856−62.
42. Jiang T, Wang Z, Proctor G, Moskowitz S, Liebman SE, Rogers T, et al. Diet-induced obesity in C57BL/6J mice causes increased renal lipid accumulation and glomerulosclerosis *via* a sterol regulatory element-binding protein-1c-dependent pathway. *J Biol Chem* 2005; **280**:32317−25.
43. Yamamoto T, Takabatake Y, Takahashi A, Kimura T, Namba T, Matsuda J, et al. High-fat diet-induced lysosomal dysfunction and impaired autophagic flux contribute to lipotoxicity in the kidney. *J Am Soc Nephrol* 2017;**28**:1534−51.
44. Luo Y, Wu MY, Deng BQ, Huang J, Hwang SH, Li MY, et al. Inhibition of soluble epoxide hydrolase attenuates a high-fat diet-mediated renal injury by activating PAX2 and AMPK. *Proc Natl Acad Sci U S A* 2019;**116**:5154−9.
45. Stachowicz A, Suski M, Olszanecki R, Madej J, Okoń K, Korbut R. Proteomic analysis of liver mitochondria of apolipoprotein E knockout mice treated with metformin. *J Proteomics* 2012;**77**:167−75.
46. Stachowicz A, Wiśniewska A, Kuś K, Kiepura A, Gębska A, Gajda M, et al. The influence of trehalose on atherosclerosis and hepatic steatosis in apolipoprotein E knockout mice. *Int J Mol Sci* 2019;**20**:1552.
47. Betz MJ, Enerbäck S. Targeting thermogenesis in brown fat and muscle to treat obesity and metabolic disease. *Nat Rev Endocrinol* 2018;**14**:77−87.
48. Busiello RA, Savarese S, Lombardi A. Mitochondrial uncoupling proteins and energy metabolism. *Front Physiol* 2015;**6**:36.
49. Childress ES, Alexopoulos SJ, Hoehn KL, Santos WL. Small molecule mitochondrial uncouplers and their therapeutic potential. *J Med Chem* 2018;**61**:4641−55.
50. Sreedhar A, Zhao Y. Uncoupling protein 2 and metabolic diseases. *Mitochondrion* 2017;**34**:135−40.
51. Geisler JG. 2,4 Dinitrophenol as medicine. *Cells* 2019;**8**:280.
52. Goedeke L, Peng L, Montalvo-Romeral V, Butrico GM, Dufour S, Zhang XM, et al. Controlled-release mitochondrial protonophore (CRMP) reverses dyslipidemia and hepatic steatosis in dysmetabolic nonhuman primates. *Sci Transl Med* 2019;**11**:eaay0284.
53. Perry RJ, Kim T, Zhang XM, Lee HY, Pesta D, Popov VB, et al. Reversal of hypertriglyceridemia, fatty liver disease, and insulin resistance by a liver-targeted mitochondrial uncoupler. *Cell Metab* 2013;**18**:740−8.
54. Samuel VT, Shulman GI. Nonalcoholic fatty liver disease as a nexus of metabolic and hepatic diseases. *Cell Metab* 2018;**27**:22−41.
55. Li SL, Yan J, Zhang YQ, Zhen CL, Liu MY, Jin J, et al. Niclosamide ethanolamine inhibits artery constriction. *Pharmacol Res* 2017;**115**: 78−86.
56. Wei YY, Xuan XC, Zhang XY, Guo TT, Dong DL. Niclosamide ethanolamine induces trachea relaxation and inhibits proliferation and

migration of trachea smooth muscle cells. *Eur J Pharmacol* 2019;**853**:229−35.
57. Hu N, Fu Y, Li WF, Yang XR, Cao M, Li FF, et al. Chemical mitochondrial uncouplers share common inhibitory effect on NLRP3 inflammasome activation through inhibiting NFκB nuclear translocation. *Toxicol Appl Pharmacol* 2021;**414**:115426.
58. Anderson VR, Curran MP. Nitazoxanide: a review of its use in the treatment of gastrointestinal infections. *Drugs* 2007;**67**:1947−67.
59. Chalasani N, Younossi Z, Lavine JE, Diehl AM, Brunt EM, Cusi K, et al. The diagnosis and management of non-alcoholic fatty liver disease: practice guideline by the american association for the study of liver diseases, american college of gastroenterology, and the American gastroenterological association. *Hepatology* 2012;**55**:2005−23.
60. Wu W, Zhao L, Yang P, Zhou W, Li B, Moorhead JF, et al. Inflammatory stress sensitizes the liver to atorvastatin-induced injury in ApoE$^{-/-}$ mice. *PLoS One* 2016;**11**:e0159512.
61. Duran A, Hernandez ED, Reina-Campos M, Castilla EA, Subramaniam S, Raghunandan S, et al. P62/SQSTM1 by binding to vitamin D receptor inhibits hepatic stellate cell activity, fibrosis, and liver cancer. *Cancer Cell* 2016;**30**:595−609.
62. Lee DH, Park JS, Lee YS, Han J, Lee DK, Kwon SW, et al. SQSTM1/p62 activates NFE2L2/NRF2 *via* ULK1-mediated autophagic KEAP1 degradation and protects mouse liver from lipotoxicity. *Autophagy* 2020;**16**:1949−73.
63. Zhang YN, Fowler KJ, Hamilton G, Cui JY, Sy EZ, Balanay M, et al. Liver fat imaging—a clinical overview of ultrasound, CT, and MR imaging. *Br J Radiol* 2018;**91**:20170959.
64. Murphy JR, Friedmann JC. Pre-clinical toxicology of nitazoxanide—a new antiparasitic compound. *J Appl Toxicol* 1985;**5**:49−52.
65. Rajoli RKR, Pertinez H, Arshad U, Box H, Tatham L, Curley P, et al. Dose prediction for repurposing nitazoxanide in SARS-COV-2 treatment or chemoprophylaxis. *Br J Clin Pharmacol* 2021;**87**:2078−88.